Vol. 24, No. 1(2025) Bio24366
Revista Mexicana de Ingeniería Química

A kinetic dynamic model of a photobioreactor in batch operation for production as biofertilizer

Modelo cinético dinámico de un fotobiorreactor en operación por lote para la producción de un biofertilizante

M.I. Sánchez-Contreras[1], R.I. Beltrán-Hernández[1], C.A. Lucho-Constantino[1], P.A. López-Pérez[2]*
[1]Centro de Investigaciones Químicas. Universidad Autónoma del Estado de Hidalgo. Carretera Pachuca-Tulancingo Km 4.5. C.P. 42184. Pachuca de Soto, Hidalgo, México.
[2]Escuela Superior de Apan. Universidad Autónoma del Estado de Hidalgo. Carretera Apan-Calpulalpan Km. 8. C.P. 43900. Chimalpa Tlalayote, Apan, Hidalgo, México.
Received: July 2, 2024; Accepted: September 27, 2024

Abstract
A native microbial consortium (MC) was isolated and propagated in BG11 and $BG11_0$ media to promote the growth of microalgae and cyanobacteria, respectively. Biomass, chlorophyll *a*, ammonium, light intensity, and dissolved oxygen were monitored during MC growth in a batch photobioreactor system. The MC highlighted the high production of chlorophyll *a* (11.2 mg L^{-1}) in BG11 and the potential as a biofertilizer because of its ammonium concentration (1.1-1.9 mg L^{-1}) in both media. An unstructured phenomenological kinetic model was developed by incorporating reaction rates in the photobioreactor for the state variables experimentally monitored. The kinetic model parameters were evaluated using the Marquardt-Levenberg algorithm, which is a nonlinear least square fitting method. The statistical evaluation of the model's effectiveness was performed using dimensionless efficiency coefficients and relative standard deviations. A global sensitivity analysis determined that the light intensity and specific oxygen consumption rate directly influenced the system. The proposed model is robust and suitable for optimization in laboratory-scale photobioreactors because it can represent the hydrodynamics parameter as k_La and the illumination area-operational volume of the photobioreactor, which is an advantage over current models for this type of system.
Keywords: Ammonium ion concentration, batch culture, Monte Carlo method, mass transfer coefficient, *Zea mays*, microbial consortium.

Resumen
Se aisló un consorcio microbiano nativo (CM) y se propagó en los medios BG11 y $BG11_0$ para promover el crecimiento de microalgas y cianobacterias, respectivamente. Se monitoreó la biomasa, la clorofila *a*, el amonio, la intensidad de la luz y el oxígeno disuelto durante el crecimiento del CM en un sistema de fotobiorreactor por lotes. El CM destacó la alta producción de clorofila *a* (11.2 mg L^{-1}) en BG11 y el potencial como biofertilizante debido a su concentración de amonio (1.1-1.9 mg L^{-1}) en ambos medios. Se desarrolló un modelo cinético fenomenológico no estructurado incorporando velocidades de reacción en el fotobiorreactor para las variables de estado monitoreadas experimentalmente. Los parámetros del modelo cinético se evaluaron utilizando el algoritmo de Marquardt-Levenberg, que es un método de ajuste de mínimos cuadrados no lineal. La evaluación estadística de la efectividad del modelo se realizó utilizando coeficientes de eficiencia adimensionales y desviaciones estándar relativas. Un análisis de sensibilidad global determinó que la intensidad de la luz y la tasa de consumo específico de oxígeno influyeron directamente en el sistema. El modelo propuesto es robusto y adecuado para la optimización en fotobiorreactores a escala de laboratorio, porque puede representar el parámetro hidrodinámico k_La y el área de iluminación-volumen operacional del fotobiorreactor, lo que representa una ventaja sobre los modelos actuales para este tipo de sistemas.
Palabras clave: Concentración de ion amonio, operación por lote, método Monte Carlo, coeficiente de transferencia de masa, *Zea mays*, consorcio microbiano.

* *Corresponding author. E-mail*: pablo_lopez@uaeh.edu.mx;
https://doi.org/10.24275/rmiq/Bio24366
ISSN:1665-2738, *issn-e*: 2395-8472

1 Introduction

The algae group comprises a wide range of photosynthetic organisms, including eukaryotic green algae and prokaryotes cyanobacteria. This diversity accounts the numerous applications in industries, such as biofuel, human and animal food, pharmaceuticals, and cosmetics. Additionally, these organisms have applications in agriculture as they stimulate microbial activity in the soil and maintain the available organic carbon and nutrients necessary for crop growth (Díaz-Godínez *et al*., 2024; Renuka *et al*., 2018).

The effectiveness of cyanobacteria and microalgae in agriculture has been documented based on their potential to improve plant growth, crop yields, modulation of soil microbial activity, and nutritional input. These effects have been observed under laboratory, greenhouse, and field conditions with several crops, and the photosynthetic microorganisms have been used in different ways: single strains, mixed cultures, and consortia (Ramírez-López *et al*., 2019: Renuka *et al*., 2018).

Regardless of the wide variety of photosynthetic microbial species and their widespread applications, only some of them are cultured on a large scale and mostly in open bioreactors because of limited experience with closed bioreactors, called photobioreactors (PBRs).This highlights the need for research focused on harnessing the advantages of PBRs, namely to maintain culture conditions with optimal values and minimize the risk of contamination (Legrand *et al*., 2021). The instrumentation needed to control the culture variables makes PBRs a more costly but an excellent choice for achieving substantial biomass production (productivity) as compared with open reactors. Modelling is a useful tool to predict the PBRs productivity and identify the parameters. This enables developing strategies and devices for controlling key parameters, leading to lower operational costs and increased PBR productivity (Ifrim *et al*., 2022).

There are several mathematical tools for modeling biological processes, such as nonlinear parametric adjustment techniques that have been used to model the growth of strains and microbial consortium. Time and resources can be saved by predicting process behavior instead of conducting experimental tests on all possible variations. Additionally, these algorithms can identify the optimal set of conditions that promote the consortium's growth and maintain process performance (Koutra *et al.*, 2018).

To describe the biological processes during microalgae growth on a macroscopic scale, single-factor or multi-factor black-box kinetic modeling frameworks with or without additive, interactive, or noninteractive formulations have been used. These models have allowed predicting biomass growth based on key operational parameters (*i.e.,* the type and composition of the culture medium, aeration, or CO_2 feeding), or environmental factors (*i.e.,* temperature, light, pH, and photoperiod) (Bekirogullari, *et al.,* 2020).

Some kinetic models are commonly employed to describe the growth of microalgae and tend to summarize the growth kinetics as a response variable dependent only on light irradiation because photosynthesis is the main reaction in this type of microorganism. Models with these characteristics, however, are unreliable because they do not reflect the complexity of photoautotrophic by not considering the influence of other variables. To overcome this limitation, models have been developed that consider both the distribution and absorption of light, as well as photosynthetic anabolism (Schediwy *et al.,* 2019).

The change in cell density in a photobioreactor causes a gradient of light in the system, affecting its productivity. This is why modeling well-mixed photosynthetic cultures allows for optimizing microalgae productivity (Schediwy *et al.,* 2019). Consistently, in homogeneously mixed systems, photosynthetic microorganisms recirculate between highly illuminated and dark areas, which reduces photoinhibition caused by high illumination (Ifrim *et al.,* 2022; Béchet *et al.*, 2013).

Currently, there are three types of microalgae biomass culture models that consider variations in light intensity and exposure periods. The first predicts the photosynthetic rate as a function of the average intensity to which the culture is exposed, and the second type measures how the local rate of photosynthesis is modified by considering operational variables, although increasing production overestimates light inhibition. The third type is a global dynamic model that considers biomass movement and exposure to light gradients with the computational application of fluid dynamics. All of these models, however, have focused on the effects of light as a main variable because microalgae are photosynthetic microorganisms (Scheufele *et al*., 2018; Cornet and Dussap, 2009).

When light is not a limiting factor or remains constant, microalgae growth in aqueous environments depends on their ability to absorb nutrients, such as N, P, and C, and incorporate them into their metabolism. Therefore, kinetic models are also expressed as functions of the concentration of some of these nutrients. Based on this, there are two types of models: those that relate the growth rate to the extracellular concentration of the nutrient (*e.g.,* Monod and Andrews models) and those that assume the concentration of nutrients inside the cell is vital for determining the growth rate (*e.g.,* Droop and Flynn models) (Lee *et al*., 2015). These models

have been modified, including metabolic variables such as substrate inhibition constants, cell physiology, and external substrate depletion, as in the models presented by Caperon-Mayer and Martinez-Sancho (Bekirogullari *et al.,* 2020; Lee *et al.*, 2015).

To generate information for expanding the potential benefits of PBRs, this study had three aims. First, based on experimental validation, we aimed to generate a comprehensive growth kinetic model for predicting the productivity of a MC incorporating a wide range of variables: concentrations of biomass [X_T], ammonium [NH_4^+], chlorophyll *a* [Ch], dissolved oxygen [O_2], the mass transfer coefficient [k_La], and light intensity [λ_I] variation. Second, we wanted to assess the efficiency of the model using dimensionless coefficients and to identify the key operating factors in PBRs productivity by applying a global parametric sensitivity analysis. Finally, we tried to outline the potential applications of the MC based on its chemical composition.

2 Materials and methods

2.1 Isolation and propagation of MC

Simple samples were collected from a crop field of *Zea mays* that was irrigated with well water and had an approximate area of 5 hectares located at 20°14'11.7" N and 98°55'38.9" W. Eight simple samples were collected from the pumping well (two), roots (one), soil (two), and water in the furrows (three). From each of the previously homogenized samples, a drop was observed by in an optical microscope (Motic, B3 Professional Series, China) to visually confirm the presence of photosynthetic organisms and continue with their propagation under laboratory conditions.

To acclimatize the MC under laboratory conditions, the eight field samples were propagated in two stages. In the first, three composite samples were integrated as follows: 1) two pumping well samples (SR), 2) one root sample and two soil samples (SS), and 3) three samples of water from the field furrows (SW). The composite samples were propagated in a PBR with 0.3 L a total volume and an operational volume of 0.2 L. Both culture media BG11 with $NaNO_3$ and $BG11_0$ without $NaNO_3$ were used to promote microalgae and cyanobacteria growth, respectively (Padey *et al.*, 2023). Composition of BG11 medium (g L^{-1}): 1) Micronutrients:H_3BO_3 0.00286, $MnCl_2{\cdot}4H_2O$ 0.00181, $ZnSO_4{\cdot}7H_2O$ 0.00022, $CuSO_4{\cdot}5H_2O$ 0.00008, $Co(NO_3)_2{\cdot}6H_2O$ 0.00005, $NaMoO_4{\cdot}2H_2O$ 0.00039; 2) Macronutrients: $NaNO_3$ 1.5, $NaCO_3$ 0.02, $CaCl_2{\cdot}2H_2O$ 0.036, $MgSO_4{\cdot}7H_2O$ 0.075, $K_2HPO_4{\cdot}3H_2O$ 0.04, Na_2-EDTA 0.001, Citric acid 0.006, $(NH_4)_5[Fe(C_6H_4O_7)_2]$ 0.006 (Touloupakis, *et al.,*2022).

In the second stage of propagation, it was necessary to increase the biomass in the PBR to 0.3 L of operational volume. Therefore, some composite samples were mixed to form four combined samples: SSS, SSR, SSW, and SSRW. The conditions for propagation were as follows: aeration for 24 h with a constant airflow 1.75-2 L min^{-1} photoperiod of 12:12 h (dark:light), lighting photon flux density (PPDF) 250-300 μmol Ph m^{-2} s^{-1}, temperature of 25 ± 5 °C, initial pH 7.1-7.4, a 14-day duration, in triplicate for each sample, with 5% inoculum taken in the stationary phase from both culture media (Dineshkumar *et al.*, 2018). The aim of this stage was to identify the growth phases of the MC.

2.2 Batch culture kinetics of the MC

Subsequently, the samples with the highest relative increase of biomass production (X_T/X_0) were selected to propagate them in a PBR with a total volume of 0.9 L and 0.5 L of operational volume. The configuration of the batch photobioreactor system is shown in Figure 1. Thus, we could compare the relative increase in biomass in different operational volumes. In this experiment, the response variables that were quantified were: biomass quantification (X_T), chlorophyll *a* (Ch) as a product, ammonium ion $\left(NH_4^+\right)$ as an indirect measure of nitrogenase activity, pH, dissolved oxygen (O_2) as an indirect measure of CO_2, and the intensity of light (λ_I) through the photobioreactor. The variables, techniques, and measurable kinetic aspects used for establishing the type of microorganisms present in the consortium, as well as some aspects of the MC metabolism, are listed in Table 1.

Table 1. Variables used to evaluate the photoautotrophic biological performance of the MC .

Measurable variable	Kinetic aspect	Technique or instrument	Reference
Biomass	Grow	Dry weight	(Tredici *et al.*, 2004)
Chlorophyll-*a*	Presence of photosynthetic microorganisms	Trichromatic method	(APHA, 1992)
	Microalgae maturity stage	Margalef index	(APHA, 1992)
NH_4^+	Amount of nitrogen transformed	Phenathe No. 132 C	(APHA, 1992)
Dissolved oxygen	Mass transfer coefficient	Multiparameter Hanna instrument HI9829	(Hernández-Melchor *et al.*, 2017)
Light intensity	Biomass density	Portable lux meter Hanna Instrument HI97500	(Guedes *et al.*, 2023)

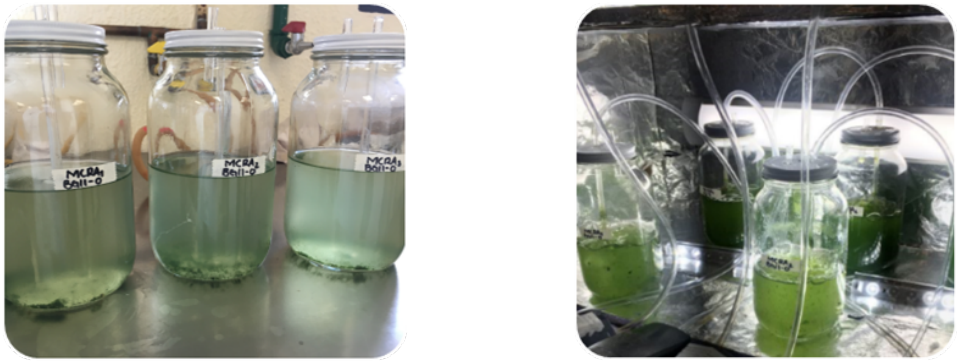

a) b)

Figure 1. Batch photobioreactor system. a) t_0 and *b*)t_7 days.

By measuring the production of chlorophyl *a* over time, we could estimate the number of photosynthetic microorganisms present in the MC (Guedes *et al*.,2023). The presence of NH_4^+ was an index of the amount of nitrogen transformed by the nitrogen-fixing microorganisms present in the $BG11_0$ medium, in addition to indicating nitrogenase inhibition, which is the enzyme responsible for nitrogen fixation (Hernández-Melchor *et al.*, 2017; Guedes *et al.*, 2023).

The relationship between the quantity of carbon dioxide absorbed from the air feed and the concentration of dissolved oxygen is complex and interrelated. Dissolved oxygen in the media allows establishing a relationship the amount of CO_2 absorbed from the air feed in the PBR, which is used by the MC in the culture medium. As carbon dioxide is absorbed into an aqueous solution, it undergoes a series of chemical reactions, forming carbonic acid and subsequently dissociating into bicarbonate and carbonate ions, which can affect the solution pH and then influence the solubility of oxygen (Grobbelaar *et al.*, 2013). During the aerobic respiration, carbon dioxide is generated and consumed for the consortium. The dissolved oxygen in the PBR is in the form that Kargi and Moo proposed as a dynamic method for calculating the volumetric coefficient of mass transfer k_La; they also represented the dispensability of all nutrients in the culture media (Hernández-Melchor *et al.*, 2017; Kazbar *et al.*, 2019).

2.3 *Analytical methods*

2.3.1 *Mechanism kinetic proposed*

A microbial consortium can provide better substrate assimilation, improved metabolite production, and resist environmental perturbations (Song *et al.,* 2024). In this context, two factors are important for the success of a reaction mechanism for a microbial consortium: nutritional factors (with the C/N ratio playing an important role in metabolism of microorganisms grown) and species compatibility, which is defined by the metabolic interactions between species. Therefore, the approach to microbial consortium kinetics has been divided into two areas: population-based modeling for the prediction of phenomenological dynamics without a detailed description of intracellular metabolism and metabolic network modeling to analyze reaction rates and their interactions in the microbial consortium (Lindemann *et al.,* 2016).

The integration of both approaches for understanding the role of interspecies interactions in regulating community dynamics is becoming increasingly important (Song *et al.,* 2014). Therefore, integrated predictive modeling approaches are required to describe the behavior of microbial consortia. In cases where reaction mechanisms have been derived through experimental studies, detailed global modeling of different reaction steps can be generated from rate expressions with symbolic forms and associated parameters (Solimeno *et al.,* 2015).

Furthermore, advances in knowledge-based design and control of microbial consortia will increasingly rely on mathematical dynamics (Song *et al.,* 2014; Solimeno *et al.,* 2015) The generality and relative ease of adaptation the model allows us to reduce the order of the state variables by considering only phenomena such as inhibition or microbial consortium (Song, 2018; Schediwy *et al.,*2019).

This research on the new dynamic model demonstrates that the high precision of all model variables is not always required, and only a few simulation outputs are significant (Silva *et al.,*2009). To model a bioprocess, after defining the structure of the reaction mechanism, it is necessary to define the interactions between the different components using mathematical expressions (López-Pérez *et al.*, 2023; Rodriguez-Mata *et al.*, 2023). The proposed mathematical model is based on the reaction mechanism present in Equation 1 (Bekirogullari *et al.*, 2020):

$$O_2 + X_T \xrightarrow[k_i]{\lambda_I} X_T + Ch + NH_4^+ \qquad (1)$$

Considerations:

- Kinetic modeling must be structured based on different sub-processes. In this work, we propose the use of a simplified metabolism model by considering the general biochemical reactions for monitoring, control, and scale-up processes below (Gasparyan *et al.,* 2020; Rao *et al.,* 2014):

Biochemical Reaction Networks ⟶ Model Reduction (2)

- Simplified model variants combine nutrient degradation and metabolites' extracellular formation based on the reaction (1).
- One single reaction (nonreversible) the reaction is under constant T, pH conditions.
- Hybrid empirical and mechanistic approach: relationship between variables, by data fitting deduced equations from a hypothetical mechanism (1).
- The kinetic rate expressions will be described based on the reaction (1) that describes the reactions using the law of mass action.
- The oxygen concentration is below inhibitory levels.

$$\mu(\delta_1,\delta_2,\ldots,\delta_n) = k_i.f(\delta_1).f(\delta_2)..f(\delta_n). \quad (3)$$

Here

$$\delta_n : O_2, X_T, Ch, NH_4^+.$$

- For simplicity, we examined microorganisms present in the consortium by using the same molecular machinery and stoichiometry to produce biomass. Thus, we understood that the rate function is universal and independent of the metabolic strategy used by a microbe to accumulate mass and energy (Gasparyan *et al.,*2020; Rao *et al.,* 2014).
- Biomass concentration is a parameter of a growth-rate function that satisfies the biologically relevant requirements that more internal resources yield faster growth.
- In general, the dynamic of the biomass considered population i in a microbial consortium can be formulated as

$$\frac{dx_i}{dt} = f(x_1, x_1, \ldots, x_n). \quad (4)$$

Here f represents a nonlinear dependence of the specific growth rate of species i, i = 1,2,..,N on population densities of other species x_i is the population density of species i. The left-hand side defines the specific growth rate of species i, and the function $f(x_1, x_2, \ldots, x_n)$, and using a Taylor expansion limited to higher order terms from (4):

$$f_{i,0} + \sum_{j=1}^{N} a_{i,j}x_j = f(x_1, x_1, \ldots, x_n) \quad (5)$$

where the interaction coefficient $a_{i,j}$ is an effect of species population j on the specific growth of species i.

If we now consider that there is no interaction between species for the purposes of this model, we have from (4) and $\sum_{j=1}^{N} a_{i,j}x_j \approx 0$

$$f_{i,0} = f(x_1, x_1, \ldots, x_n) \approx X_T, \quad (6)$$

where $f_{i,0}$ is the basal growth rate of species i, which depends on the specific culture medium to increase the growth of a certain species over others (Li *et al.*, 2024; Kaneko, 2024; Sánchez-Zurano *et al*., 2021; Jiménez-Ríos *et al*., 2024).

2.3.2 Statistical correlation coefficients

The primary objective of mathematical models is to depict a phenomenon and replicate its behavior across various conditions. Nevertheless, when constructing a model, certain assumptions and simplifications are typically made, which can lead to uncertainty about the confidence level of the model when crucial information is omitted. Therefore, it is essential to conduct an analysis that assures confidence in the proposed model (Martínez-Hilario *et al*., 2023). Utilizing statistical efficiency coefficients is helpful for offering a benchmark for the degree of congruity between the experimental data and the proposed model. Bioprocesses are subject to many variables that are routinely modified, and, thus, parametric sensitivity analysis helps establish the overall confidence of the model, by examining the uncertainties that are frequently connected with the parameters involved in the model (Alvarado-Santos *et al*., 2022; López-Pérez *et al.,* 2016).

Efficiency Coefficient (P): According to the proposition in Equation 7, the model's fit with the sample values is good, when represents a strong alignment between the model and the experimental data (Martínez-Hilario *et al*., 2023):

$$\mathbf{P=1-\frac{\sum_{i=1}^{j}(\delta_i-\theta_i)^2}{\sum_{i=1}^{j}(\delta_i-\underline{\delta})^2}} \quad (7)$$

where

- θ_i are numerical data at time t_i,
- δ_i is the experimental value at time t_i,
- $\underline{\delta}$ is the mean value of the experimental variable,

- *and* j is the data integer.

Relative Standard Deviation (RSD): This is a statistical value that represents the dispersion of data relative to the mean and standard deviation, expressed as a percentage. It is helpful for assessing the variability of measurements between different observations of variable magnitudes (Alvarado-Santos *et al.*, 2022).

2.3.3 *Parametric identification*

Generally, global optimization methods explore the parameter space more comprehensively but converge at a slower pace. Hybrid optimization methods explore the parameter space at a fast convergence rate by initiating a parameter estimation using a local method once they approach a local optimum. The objective function J in Equation 8 seeks to minimize the discrepancy between the experimental data and the simulated model values, which represent the hybrid approach depicted:

$$J = \sum_{t=0}^{t_f} \Big(\Big[O_{2\exp} - O_{2m} \Big]^2 + \Big[X_{T\exp} - X_{Tm} \Big]^2 + \Big[Ch_{\exp} - Ch_m \Big]^2 + \Big[NH_{4\,\exp}^{+} - NH_{4\,m}^{+} \Big]^2 + \Big[\lambda_{I\exp} - \lambda_{Im} \Big]^2 \Big). \quad (8)$$

For the first approximation of the model, a Marquardt-Levenberg fit and Equation 8 were used, as well as the MATLAB fminsearch function for the global and specific fit.

2.3.4 *Global parametric sensitivity analysis*

Monte Carlo simulation is a widely employed method for conducting sensitivity analysis, which entails examining the way a model reacts to randomly generated inputs and helps to increase the level of confidence in mathematical models by allowing parameter sweeps, exploring the design space, and testing various scenarios. Simulink Design Optimization^{TM} is an interactive tool for performing this sensitivity analysis and influences the design of models that are performed in a block programming environment (Simulink). We used the sampling approach of the probability density functions associated with the input variables. In this case, all parameters were changed simultaneously, and the sensitivities were calculated over the full range of variation of the input factors. This method allows the decomposition of the variance of the output using a Monte Carlo simulation. Global sensitivity indices represent the contribution of each input factor (model parameter) to the output variance (López-Pérez *et al.*, 2023; Becker *et al.*, 2018).

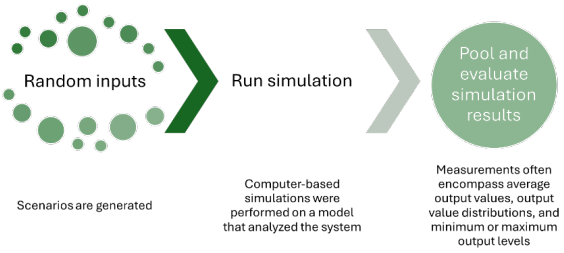

Figure 2. Steps of Monte Carlo simulation method.

Traditionally, this process has consisted of three distinct steps as shown in Figure 2 (Becker *et al.*, 2018; Rahimikhoob *et al.*, 2024).

3 Results and discussion

3.1 *Isolation and propagation of MC*

The MC growth in the composite samples during the first propagation stage was monitored qualitatively, macroscopically, and microscopically. Figure 3 shows the initial (t_0) and final (t_{21} and t_{42} for BG11 and $BG11_0$ media, respectively) appearance of the PBRs and the microscope images of MC in BG11 and $BG11_0$ media. The propagation of SS, SR, and SW occurred over 21 days in BG11 medium, but it took 42 days in $BG11_0$. This result is attributed to the time conservation of samples at 4 °C and the exclusive presence of nitrates in the BG11 medium. During conservation, the MC consumed nutrients in the samples, and, when the PBRs were inoculated, the MC had sufficient nutrients to develop in the BG11 medium, while, in the $BG11_0$, the cyanobacteria had to perform N-fixation to supply this nutrient to other consortium members.

In the second propagation stage, the biomass of the three composite samples grew 2.1 to 2.6 times in size in 14 days with the BG11 medium. Conversely, in the $BG11_0$ medium, SR and SS displayed a greater increase of 3.2 and 3.4 times in 12 days, while SW did not grow at all. The growth stages of the MC were not clearly identifiable in either of the two media. It is important to mention that biomass production is presented as the increase in initial biomass (X_T/X_0). This dimensionless criterion was objectively applied to compare the biomass production during PBRs scaling up (Lee *et al.*, 2013).

Unlike the composite samples, the combined SSR and SSRW samples presented all four phases of microbial growth: dormancy (days 0-2), exponential (days 2-10), stationary (days 10-12), and decay (after day 12).

The increase in the biomass (X_T/X_0) of SSRW in both the BG11 and $BG11_0$ media during the PBR scaling up from 0.3 to 0.5 L, which indicates that

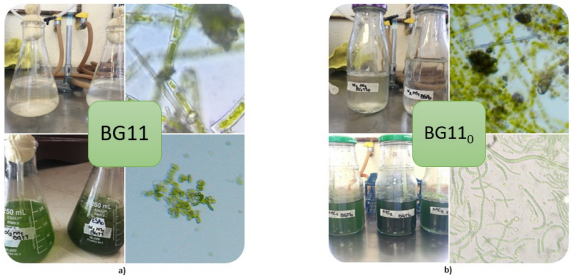

Figure 3. First stage of propagation, macroscopically and microscopically: a) BG11 media (up, t_0 *and down* t_{21}) *and b)* $BG11_0$ *media. (up,* t_0 *and down,* t_{42}).

scaling MC production to other PBR dimensions by maintaining constant culture conditions is possible.

3.2 *Batch culture kinetics of the MC in 0.5 L PBR*

The most important components for autotrophic growth are C, N, and P, and their supply is essential for the biotechnology of photosynthetic microorganisms. Limiting or providing excess energy is not a solution for increasing or reducing growth (Grobbelaar, 2013). The MC had adequate C and N concentrations, which were measured indirectly by the concentration of dissolved oxygen (O_2) and ammonium ion (NH_4^+), to produce biomass, chlorophyll *a*, and NH_4^+ in the $BG11_0$ medium.

The biomass of the MC in the $BG11_0$ medium continued to increase after 10 days, but the production of chlorophyll *a* started to decline, indicating a decrease in the growth rate of photosynthetic microorganisms. One possible explanation is that in batch culture the rise in cell density hinders the amount of light energy reaching the culture surface (Lee et al., 2013). The growth of nonphotosynthetic species in the MC could explain the increase in biomass. Similarly, the inorganic carbon in the medium started to decrease noticeably after 10 days as the biomass grew. Regarding the nitrogen present, the NH_4^+ content increased from day 4 onwards, indirectly indicating the nitrogenase activity of cyanobacteria in converting atmospheric nitrogen to ammonium ions (Carletti *et al.*, 2024; Dobrojan *et al.*, 2023). Nutrient consumption depends on all factors that influence microalgae growth, such as light, temperature, aeration, turbulence, and the culture medium (Grobbelaar, 2013).

The increase in the proportion of biomass and chlorophyll-*a* production in the BG11 medium. The behavior of MC in the BG11 culture medium varied considerably in terms of chlorophyll-*a* production, as it reached 12 mg L^{-1}, which is comparable to the amounts produced by pure strains. As with the $BG11_0$ medium on day 12, the biomass proportion increased as the chlorophyll-*a* concentration decreased, indicating a decline in the growth rate of photosynthetic microorganisms in the MC.

In this case, the increase in the concentration of NH_4^+ in the medium could be caused by the conjugation of different metabolic routes of the microalgae and cyanobacteria present in the MC; in the end, had a higher concentration than in the $BG11_0$ medium, as previously mentioned (Carletti *et al.*, 2024; Dobrojan *et al.*, 2023).

3.3 *Numerical studies*

3.3.1 *Proposed model*

MATLAB® Simulink software was utilized to simulate equations (9-13), employing the numerical method of ode45 with a fixed step size of 0.001. Moreover, specific initial conditions were set for the simulation: O_2 = 4.7 mg L^{-1}, X_T = 100 mg L^{-1}, Ch = 0.14 mg L^{-1}, NH_4^+ = 0.41 mg L^{-1} for λ_I = 69 μmol Ph m^{-2} s^{-1} and O_2 = 5.5 mg L^{-1}, X_T = 1700 mg L^{-1}, Ch = 0.1 mg L^{-1}, NH_4^+ = 0.37 mg L^{-1} for λ_I=69 μmol Ph m^{-2} s^{-1} to $BG11_0$ and BG11 cultures, respectively.

The proposed model can provide correct simulations by using the 14 parameters of Table 2. The degree of fit between the proposed model and the experimental data is evaluated by utilizing statistical coefficients of efficiency, as demonstrated in Table 3. The model's ability to describe the experimental observations related to discontinuous kinetics is quantified by applying the statistical correlation criteria, including the R^2 (correlation coefficient) and E (efficiency coefficient).

3.3.2 *Mass balance equations*

$$\text{Dissolved oxygen } (O_2): \frac{dO_2}{dt} = -k_1\varphi X_T + k_L a\left[O_2^* - O_2\right] \quad (9)$$

$$\text{Biomass } (X_T): \frac{dX_T}{dt} = k_2\theta X_T O_2 - k_3\lambda_I X_T \quad (10)$$

$$\text{Chlorophyll } a \ (Ch): \frac{dCh}{dt} = k_4 Ch^{\delta} X_T \lambda_I \quad (11)$$

$$\text{Ammonium ion } \left(NH_4^+\right) \frac{dNH_4^+}{dt} = k_5 NH_4^+ X_T \varphi\, \theta \quad (12)$$

$$\text{Light irradiation } (\lambda_I) \frac{d\lambda_I}{dt} = -k_6\theta X_T \gamma \quad (13)$$

Here

Irradiation light term

$$\theta = \left[1 - \frac{\lambda_I}{k_7}\right]^{\alpha} \quad (14)$$

Table 2. Kinetic parameters reported for pure strains and mixed cultures versus values calculated in proposed model.

Symbol	Mean	Value BG11	Value $BG11_0$	Interval reported in literature	Reference
$\mathbf{k_1}$	Specific dissolved oxygen rate (d^{-1})	$5.73E-5 \pm 1.02E-5$	$4.1E-5 \pm 2E-5$	$[4.9E-6 - 9.6E-9]$	(Hernández-Melchor *et al.*,2017; Kazbar *et al.*, 2019; Reyna-Velarde *et al.*, 2010)
$\mathbf{k_2}$	Cell formation coefficient (d^{-1})	0.89 ± 0.2	0.70 ± 0.18	[0.14 – 2.3]	(Koller *et al.*, 2017)
$\mathbf{k_3}$	Inhibition constant of biomass density ($d^{-1}\mu mol^{-1}\ Ph^{-1}m^{2}\ s$)	$21E-4 \pm 10E-4$	$15E-4 \pm 10E-4$	[0.0001 – 0.0008]	(Bekirogullari *et al.*,2020; Povis *et al.*2024)]
$\mathbf{k_4}$	Constant reaction rate of chlorophyll *a* (d^{-1})	0.175 ± 0.09	0.35 ± 0.1	[0.1 – 0.3]	(Bekirogullari *et al.*,2020)
$\mathbf{k_5}$	Constant reaction rate of NH_4^+ (d^{-1})	5.1 ± 3	4.5 ± 2	[0.014 – 2.99]	(Koller *et al.*, 2017)
$\mathbf{k_6}$	Constant reaction rate of irradiation light ($\mu mol\ Ph\ m^{-2}s^{-1}d^{-1}$)	6.6 ± 1	5.1 ± 1.5	[0.32 – 21.3]	(Guedes *et al.*, 2023; Koller *et al.*, 2017)
$\mathbf{k_7}$	Inhibition constant irradiation light $\left(\mu mol\ Ph\ m^{-2}s^{-1}\right)$	15.5 ± 4	12 ± 3	[1 – 20]	(Guedes *et al.*, 2023; Koller *et al.*, 2017)
$\mathbf{k_8}$	Inhibition constant dissolved oxygen ($mg\ L^{-1}$)	6.7 ± 2	4.9 ± 1.5	[1 – 10]	(Hernández-Melchor *et al.*,2017; Reyna-Velarde *et al.*, 2010)
$\mathbf{k_La}$	Mass transfer coefficient (d^{-1})	$4E-4 \pm 1E-4$	$5E-4 \pm 0.15E-4$	[5.52 – 1130]	(Hernández-Melchor *et al.*,2017; Kazbar *et al.*, 2019)
$\mathbf{Y}$	Biomass yield due to oxygen consumption	0.45 ± 0.1	0.6 ± 0.3	[0.1 – 1]	(Guedes *et al.*, 2023; Koller *et al.*, 2017)
$\mathbf{Y}_1$	Biomass yield due to irradiation light	0.35 ± 0.1	0.5 ± 0.2	[0.1 – 1]	(Guedes *et al.*, 2023; Koller *et al.*, 2017)
α	Exponent of the irradiation light (dimensionless)	1.5 ± 0.2	1.0 ± 0.4	[1 – 10]	(Guedes *et al.*, 2023; Koller *et al.*, 2017)
β	Exponent of the dissolved oxygen (dimensionless)	0.5 ± 0.2	0.7 ± 0.3	[0.1 – 3]	(Guedes *et al.*, 2023)
γ	Constant area-volume ratio	12 ± 2.5	10 ± 3.5	–––––	––

Dissolved oxygen term

$$\varphi = \left[\frac{O_2}{k_{8+O_2}}\right]^{\beta} \tag{15}$$

Ratio illumination area / operational volume

$$\gamma = \frac{A_i}{V_o}. \tag{16}$$

Here, $\pi = [k_1,\ k_2, k_3,\ k_4, k_5, k_6, k_7, k_8, k_La\ ]$ are the reaction rates (k_i), and k_3 is the inhibition constant for X_T , which is the biomass density in the PBR. π is a parameter vector is a named numeric vector (the parameter values).

The proposed model's strength lies in its ability to quantitatively correlate biomass increase with two significant aspects of the MC: chlorophyll-*a* concentration indicating the presence of photosynthetic microorganisms and the production of ammonium ions resulting from nitrogen fixation activity. Equation (1) describes the oxygen balance during transfer from an air bubble to the culture medium and consumption by the MC. Furthermore, because CO_2 is the carbon source for biomass production and N is necessary for maximum biomass production, coupling the O_2 (air flow) variable to the model facilitates the determination of the optimal mass transfer coefficient for maximum biomass production.

In natural environments, there is a co-limitation by the light or different nutrients, which assumes that for photosynthetic microorganisms their growth depends on the interactions between nutrients and light (Schediwy *et al.,* 2019). The reported models have been based on the hypothesis that the growth rate is affected by the rarest nutrient found in the least amount: limiting. Thus, it appears to be a single-factor kinetic model. The premise of this type of kinetic model is that the maximum growth rate $\mu_{\max}$ is calculated for the most limiting nutrient, whereas for other models $\mu_{\max}$ it is a function of both limiting nutrients (*e.g.,* P and N) and the other limiting resources (*e.g.,* CO_2, and light intensity) (Schediwy *et al.,* 2019; Scheufele *et al*., 2018).

Each aspect of mass balance must be explicitly expressed as a set of kinetic equations to define a mathematical model that represents the interactions between different components of the system (López-Pérez *et al.*, 2023; Alvarado-Santos *et al.*,2023; Romero Cortes *et al.*, 2018) From these criteria, it was determined that the model accurately represented the experimental data; see Figures 4 and 5.

The advantages and considerations of the proposed model are described below.

The key advantage of the proposed kinetic modeling method is that it quantitatively evaluates the elements that dictate the concentration levels of the primary metabolites in a photobioreactor, thereby providing a more accurate representation of the process.

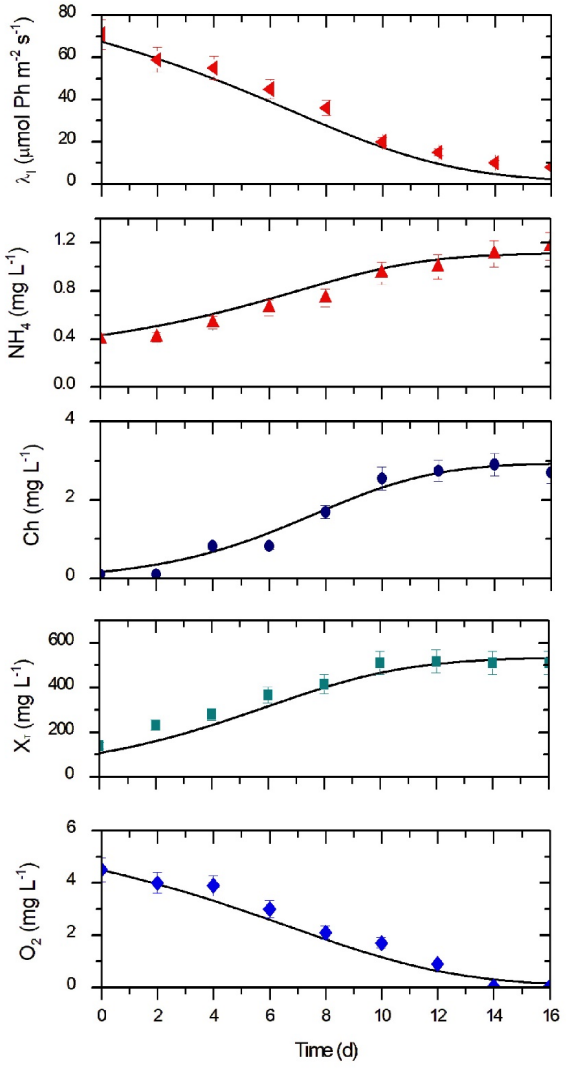

Figure 4. Predictive capacity of the developed mathematical model. Model predictions (lines) experimental data (symbols) in the $BG11_0$ medium.

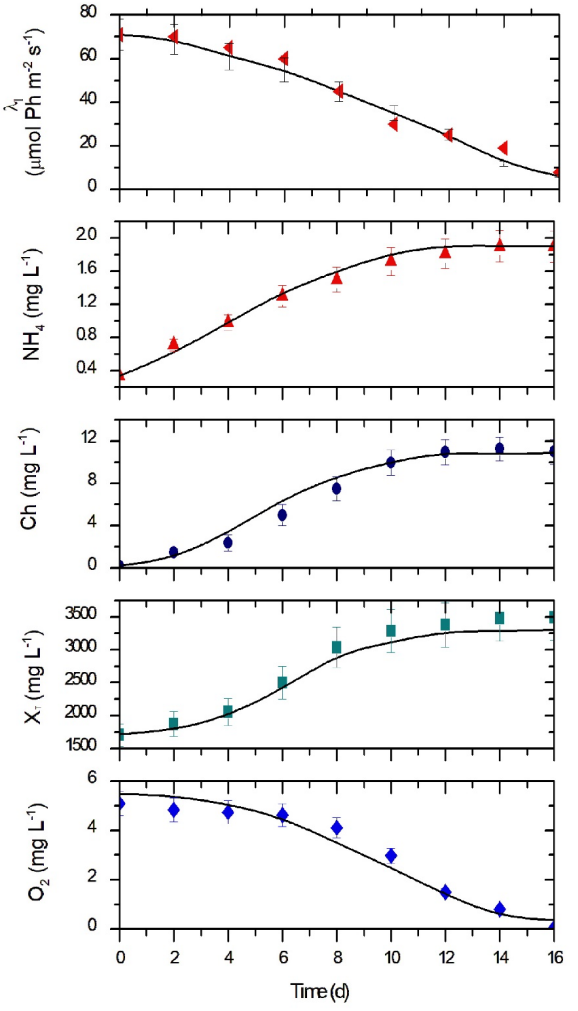

Figure 5. Predictive capacity of the developed mathematical model. Model predictions (lines) experimental data (symbols) in the BG11 medium.

The principles of kinetic modeling apply to the extracellular environment of a microbial consortium. The proposed kinetic model can explain the rates of dissolved oxygen, biomass, chlorophyll *a*, ammonium ions, and light irradiation, as well as the metabolic interactions associated with these variables. Furthermore, it has the ability to make predictions under different initial experimental conditions, which has not been considered in many studies (Bekirogullari *et al*., 2020).

In addition, compared with the models reported in the literature, ours includes information about the ratio of illumination area/operational volume and k_La, which were decisive parameters for the scaling and viability of the bioprocess. In this model, the vector constants k_i were assumed to remain constant and uninfluenced by external factors throughout the procedure.

The conversion rate of each component in the proposed Equation 1 will depend on the ratio between the initial concentrations and the reaction rate constant, as well as the shape of the kinetic curve and its plot, as determined by Equations 9 to 16.

3.3.3 Parametric sensitivity analysis

The Monte Carlo method was applied to differentiate the most sensitive parameters that affect the model's output variables including biomass, chlorophyll *a*, ammonium concentration, light intensity, and dissolved oxygen by using a tornado chart of a one-way sensitivity analysis. A Monte Carlo of partial correlation and standardized regression for every parameter were respectively implemented in the sensitivity analysis for 14 kinetic parameters relating to the model's variables. The values were obtained by 10,000 Monte Carlo simulations around ±15% the best fit values experimental data.

Table 3. Statistical correlation coefficients.

Variable	BG11		$BG11_0$	
	R^2	P	R^2	P
Dissolved oxygen (O_2)	0.949	0.978	0.954	0.967
Biomass (X_T)	0.964	0.979	0.959	0.972
Chlorophyll *a* (Ch)	0.936	0.951	0.976	0.985
Ammonium ion (NH_4^+)	0.988	0.995	0.983	0.998
Light irradiation λ_I	0.975	0.981	0.969	0.981
Average	0.962	0.976	0.968	0.980

The model's global sensitivity analysis indicated that it is primarily sensitive to dynamics of $O_2 \gg \lambda_I \gg NH_4^+ > X_T > Ch$, which are based on the sources of carbon and energy for photosynthetic metabolism (Povis *et al*., 2024). For instance, each bar of the tornado chart correlates to an independent uncertain parameter.

Figure 6a shows the effect of the parameters on the concentration of dissolved oxygen:

$$O_2 : \begin{cases} \pi < 0, \left\{ \overrightarrow{\beta > k_8 > \gamma > k_7 > k_6 > Y > k_4} \right\} \\ \pi > 0, \left\{ \overrightarrow{k_1 > k_3 > k_2 > k_L a > k_5 > Y_I > \alpha} \right\} \end{cases} . \tag{17}$$

Definition a show that the β, k_8, γ exponent of the dissolved oxygen, inhibition constant dissolved oxygen, and the constant area-volume ratio had strong positive correlations in the dynamic dissolved oxygen, whereas the k_1, k_3, $k_2, k_L a$ of these parameters Specific dissolved oxygen rate, Cell formation coefficient, Inhibition constant of biomass density and Mass transfer coefficient had significant negative correlations.

Figure 6b shows the effect of the parameters on the concentration of biomass:

$$X_T : \begin{cases} \pi < 0, \left\{ \overrightarrow{Y_I > k_3 > Y > k_8 > k_2 > k_5 > k_4 > k_L a} \right\} \\ \pi > 0, \left\{ \overrightarrow{\alpha > \gamma > k_7 > k_1 > \beta > k_6} \right\} \end{cases} . \tag{18}$$

Definition a show that Y_I, k_3, Y biomass yield caused by irradiation light, the inhibition constant of biomass, and the biomass yield from oxygen consumption had strong positive correlations in the dynamic biomass, whereas the $\alpha > \gamma > k_7$ of these parameters had significant negative correlations.

Figure 6c shows the effect of the parameters on the concentration of chlorophyll *a*

$$Ch : \begin{cases} \pi < 0, \left\{ \overrightarrow{k_1 > k_2 > k_7 > \gamma > k_L a > k_3 > \alpha} \right\} \\ \pi > 0, \left\{ \overrightarrow{k_8 > k_6 > Y_I > k_4 > Y > \beta > k_5} \right\} \end{cases} \tag{19}$$

Definition a shows that the k_1, k_2, k_7 parameters' ratio had strong positive correlations with the dynamic dissolved oxygen, whereas the k_8, k_6, Y_I of these parameters had significant negative correlations.

Figure 6d shows the effect of the parameters on the concentration of ammonium:

$$NH_4^+ : \begin{cases} \pi < 0, \left\{ \overrightarrow{\beta > k_7 > k_6 > \gamma > k_8 > k_2 > Y_I > \alpha} \right\} \\ \pi > 0, \left\{ \overrightarrow{k_5 > k_3 > k_4 > k_1 > Y > k_L a} \right\} \end{cases} . \tag{20}$$

Definition a show that the β, k_7, k_6 parameters had strong positive correlations in the dynamic ammonium, whereas the k_5, k_3, k_4 of these parameters had significant negative correlations.

Figure 6e shows the effect of the parameters on the concentration of light intensity:

$$\lambda_I : \begin{cases} \pi < 0, \left\{ \overrightarrow{\beta > k_7 > k_8 > \gamma > k_6 > k_5} \right\} \\ \pi > 0, \left\{ \overrightarrow{k_1 > k_3 > Y_I > k_L a > k_2 > \alpha > k_4 > Y} \right\} \end{cases} . \tag{21}$$

Definition a show that the β, k_7, k_8 parameters had strong positive correlations in the dynamic light intensity, whereas the k_1, k_3, Y_I of these parameters had significant negative correlations.

In general, the concentration of dissolved oxygen is then strongly related to the constants k_1 and k_8 involved in the consumption of carbon dioxide. Moreover, it strongly correlates with k_3 and γ, which signifies growth inhibition based on the MC's light exposure. Biomass accumulation hinders light transmission in the photobioreactor, and gamma radiation calculates the illuminated area to volume ratio (Béchet *et al.,*2013). A sensitivity analysis was performed on the model to infer which parameters have the most influence to the extent in which the model becomes unstable. The behavior of the parameters was the same for the MC models in BG11 and $BG11_0$. The model's global sensitivity analysis indicated that it was primarily sensitive to O_2 (an indirect measure of CO_2) and λ_I, aligning with the sources of carbon and energy for photosynthetic metabolism (Povis *et al*., 2024).

Finally, a classic scaling criterion is the geometric similarity ratio between the different scales: the percentages between the main reactor sizes. Geometric restrictions, however, do not guarantee the same conditions at all scales, so the operating parameters must also be modified. The proposed model assessed,

apart from the geometric criterion (γ), the mass transfer coefficient (k_La), which was physically related to the concentration of dissolved oxygen, substrate, and mixing time and caused the development of gradients that significantly affect biomass growth (Cappello 2020).

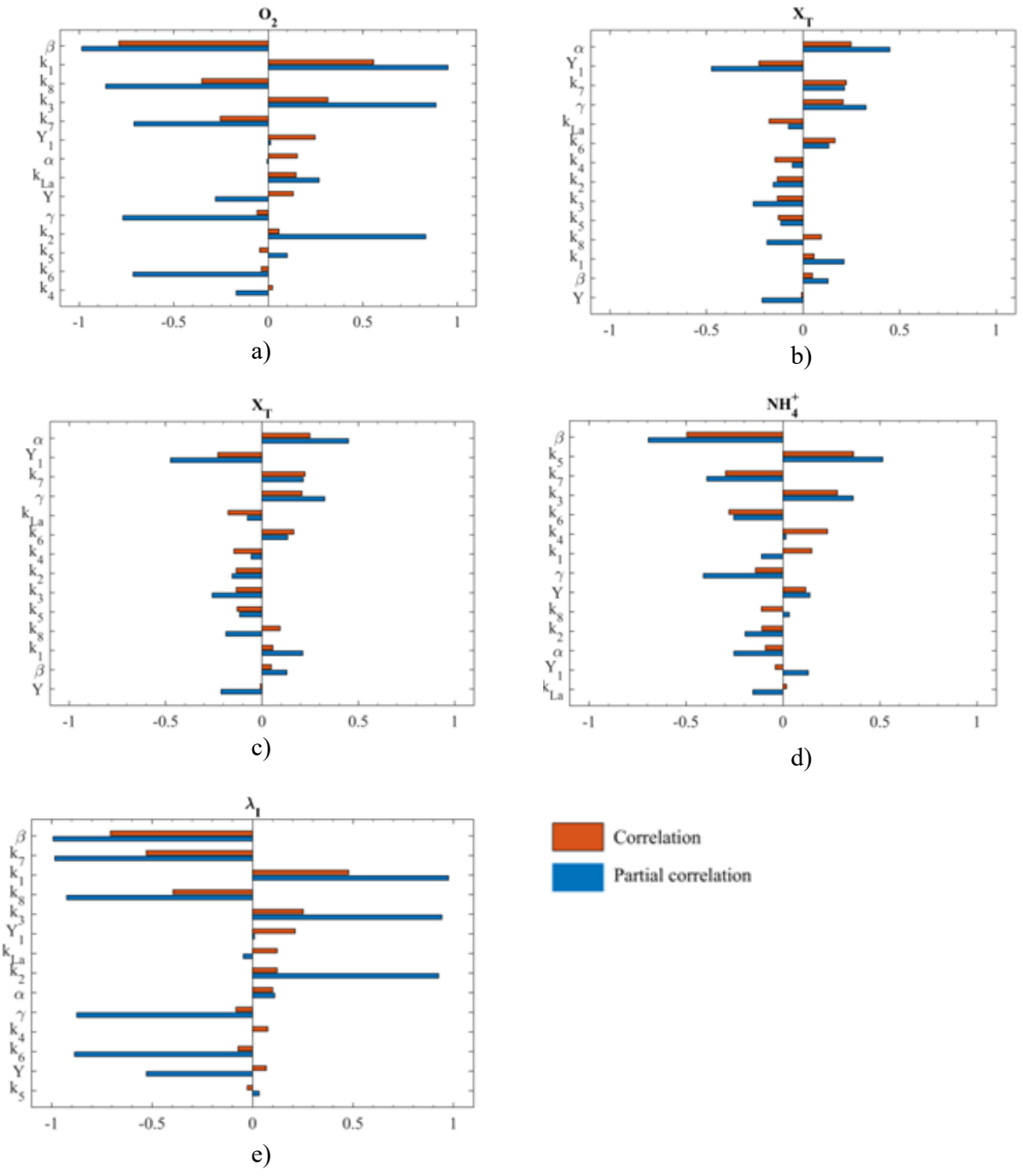

Figure 6. Sensitivity analysis of the constants of the inhibition model and MC production.

Conclusion

This study focused on creating and evaluating a model to represent the growth of a MC, which involved an important number of meaningful variables of photosynthetic growth in two culture media in a photobioreactor with aeration in batch operation. The experimental data indicated the potential of the MC as a biofertilizer because of its NH_4^+ content, which is one of the forms of nitrogen assimilable by plants. In the BG11 medium, the MC showed promise as a chlorophyll-*a* producer,

comparable to pure strains. The new kinetic model proposed provides an experimental prediction in real cases. The optimized parameters from the Levenberg-Marquardt algorithm matched the experimental data exceptionally well, especially in comparison to the simulations. The RSD and P values indicated that the model predictions, based on experimental observations, performed satisfactorily. The global-scale parametric sensitivity analysis, conducted using the Monte Carlo approach, revealed that the light intensity and specific oxygen consumption rate had the most significant impact on the model. The proposed model is it can represent the parameters and the area-operational volume related to hydrodynamics of the photobioreactor. Finally, we find that this approach provides a mathematical description of the photobioreactor for optimization and control.

Symbols

X_T	Biomass mg L^{-1} P
O_2	Dissolved oxygen mg L^{-1}
NH_4^+	Ammonium ion mg L^{-1}
λ_I	Light irradiation μmol Ph $m^{-2}s^{-1}$
θ	Irradiation light term
φ	Dissolved oxygen term
γ	Ratio illumination area /operational volume m^{-1}

Acknowledgements

M.I. Sánchez-Contreras acknowledges the Humanities, Sciences and Technology National Council (CONAHCYT) for the doctoral scholarship no 761776 granted to her for the development of this work.

References

Alvarado-Santos, E., Aguilar-López, R., Neria-González, M.I., Romero-Cortés, T., Robles-Olvera, V.J., and López-Pérez, P.A. (2023). A novel kinetic model for a cocoa waste fermentation to ethanol reaction and its experimental validation. *Preparative Biochemistry and Biotechnology*, *53*(2), 167-182. https://doi.org/10.1080/10826068.2022.2056746

Alvarado-Santos, E., Mata-Machuca, J.L., López-Pérez, P.A., Garrido-Moctezuma, R.A., Pérez-Guevara, F., and Aguilar-López, R. (2022). Comparative analysis of a family of sliding mode observers under real-time conditions for the monitoring in the bioethanol production. *Fermentation*, 8(9), 446. https://doi.org/10.3390/fermentation8090446

American Public Health Association (1992). American Water Works Association, and Water Environment Federation. 8110 In *Standard Methods for the Examination of Water and Wastewater*. Lipps, W.C.; Baxter, T.E.; Braun-Howland, E. (Eds.) APHA Press.

American Public Health Association (1992). American Water Works Association, and Water Environment Federation. 4500-NH_3 nitrogen (ammonia), In *Standard Methods for the Examination of Water and Wastewater*. Lipps, W.C.; Baxter, T.E.; Braun-Howland, E. (Eds.) APHA Press.

Béchet, Q., Shilton, A., and Guieysse, B. (2013). Modeling the effects of light and temperature on algae growth: state of the art and critical assessment for productivity prediction during outdoor cultivation. *Biotechnology Advances*, 31(8), 1648-1663. https://doi.org/10.1016/j.biotechadv.2013.08.014

Becker, W.E., Tarantola, S., and Deman, G. (2018). Sensitivity analysis approaches to high-dimensional screening problems at low sample size. *Journal of Statistical Computation and Simulation*, 88(11), 2089-2110. https://doi.org/0.1080/00949655.2018.1450876

Bekirogullari, M., Figueroa-Torres, G.M., Pittman, J.K., and Theodoropoulos, C. (2020). Models of microalgal cultivation for added-value products-A review. *Biotechnology Advances*, 44, 107609. https://doi.org/10.1016/j.biotechadv.2020.107609

Cappello, V., Scale-up of gas-liquid agitated bioreactors Three-dimensional modeling of hydrodynamics, mass transfer and kinetics. Chemical and Process Engineering. Université Clermont Auvergne, 2020.

Carletti, M., Barbera, E., Filippini, F., and Sforza, E. (2024). Effect of ammonium/nitrate ratio on microalgae continuous cultures: Species-specificity of nutrient uptake and modelling perspectives. *Journal of Water Process Engineering*,58, 104762. https://doi.org/10.1016/j.jwpe.2023.104762

Cornet, J. F., and Dussap, C. G. (2009). A simple and reliable formula for assessment of maximum volumetric productivities in photobioreactors. *Biotechnology Progress*, 25(2), 424-435. https://doi.org/10.1002/btpr.138

Díaz-Godínez, G. Peña-Solis, K., and Díaz-Domínguez, G. (2024). Algae as nutritional and bioactive food ingredients. *Revista Mexicana de Ingeniería Química* 23, Bio24209 https://doi.org/10.24275/rmiq/Bio24209

Dineshkumar, R., Kumaravel, R., Gopalsamy, J., Azim, S. N. M. and Sampathkumar, P. (2018). Microalgae as bio-fertilizers for rice growth and seed yield productivity. *Waste Biomass Valor* 9, 793-800. https://doi.org/10.1007/S12649-017-9873-5.

Dobrojan, S., Jigău, G., and Dobrojan, G. (2023). Nitrogen fixing cyanobacteria-regulators of nitrogen content. *Present Environment and Sustainable Development*, (1), 48-50.

Gasparyan, M., Van Messem, A., and Rao, S. (2020). An Automated Model Reduction Method for Biochemical Reaction Networks. *Symmetry*, 12, 1321. https://doi.org/10.3390/sym12081321

Grobbelaar, J.U. (2013) Inorganic Algal Nutrition. In *Handbook of Microalgal Culture: Applied Phycology and Biotechnology*. Hu, Q.; Richmond, A. (Eds.) Wiley Blackwell. 123-133. https://doi.org/10.1002/9781118567166

Guedes, V.C., Palma, G.M., and Horta, A.C.L. (2023). An evaluation of light wavelengths, intensity and control for the production of microalgae in photobioreactors: a review. *Brazilian Journal of Chemical Engineering*, 1-14. https://doi.org/10.1007/s43153-023-00388-x

Hernández-Melchor, D.J., Cañizares-Villanueva, R.O., Terán-Toledo, J.R., López-Pérez P.A., and Cristiani-Urbina, E. (2017). Hydrodynamic and mass transfer characterization of flat-panel airlift photobioreactors for the cultivation of a photosynthetic microbial consortium. *Biochemical Engineering Journal*, 128, 141-148. https://doi.org/10.1016/j.bej.2017.09.014

Ifrim, G. A., Titica, M., Horincar, G., Antache, A., Baicu, L., Barbu, M., and Guzmán, J.L. (2022). Model based optimal control of the photosynthetic growth of microalgae in a batch photobioreactor. *Energies*, 15(18), 6535. https://doi.org/10.3390/en15186535

Jiménez-Ríos, L., Torrado, A., González-Pimentel, J. L., Iniesta-Pallarés, M., Molina-Heredia, F. P., Mariscal, V., and Álvarez, C. (2024). Emerging nitrogen-fixing cyanobacteria for sustainable cotton cultivation. *Science of the Total Environment*,*924*, 171533. https://doi.org/10.1016/j.scitotenv.2024.171533

Kaneko, K. (2024). Constructing universal phenomenology for biological cellular systems: an idiosyncratic review on evolutionary dimensional reduction. *Journal of Statistical Mechanics: Theory and Experiment*, (2), 024002.https://doi.org/10.1088/1742-5468/ad1f54

Kazbar, A., Cogne, G., Urbain, B., Marec, H., Le-Gouic, B., Tallec, J., and Pruvost, J. (2019). Effect of dissolved oxygen concentration on microalgal culture in photobioreactors. *Algal Research*, 39, 101432. https://doi.org/10.1016/j.algal.2019.101432

Koller, A.P., Löwe, H., Schmid, V., Mundt, S., and Weuster-Botz, D. (2017). Model-supported phototrophic growth studies with Scenedesmus obtusiusculus in a flat-plate photobioreactor. *Biotechnology and Bioengineering*, 114(2), 308-320. https://doi.org/10.1002/bit.26072

Koutra, E., Economou, C. N., Tsafrakidou, P., and Kornaros, M. (2018). Bio-based products from microalgae cultivated in digestates. *Trends in Biotechnology*, 36(8), 819-833. https://doi.org/10.1016/j.tibtech.2018.02.015

Lee, E., Jalalizadeh, M., and Zhang, Q. (2015) Growth kinetic models for microalgae cultivation: A review. *Algal Research*, 12, 497-512. https://doi.org/10.1016/j.algal.2015.10.004.

Lee, S. K.; Lur, H. S.; Liu, C.-T. (2021) From lab to farm: elucidating the beneficial roles of photosynthetic bacteria in sustainable agriculture. *Microorganisms*, *9*, 2453. https://doi.org/10.3390/microorganisms9122453

Lee, Y., Chen, W., Shen, H., Han, D., Li, Y., Jones, H.D.T., TimLin, J.A. and Hu, Q. (2013). Basic culturing and analytical measurement techniques. In *Handbook of Microalgal Culture: Applied Phycology and Biotechnology.* Hu, Q.; Richmond A. (Eds.) Wiley Blackwell., 37-68. https://doi.org/10.1002/9781118567166.ch3

Legrand, J., Artu, A., and Pruvost, J. (2021). A review on photobioreactor design and modelling for microalgae production. *Reaction Chemistry & Engineering*. https://doi.org/10.1039/d0re00450b

Li, J., Tosino, H.S., Ladewig, B.P., Jung, N., Bräse, S., and Dittmeyer, R. (2024). Extraction of the intrinsic rate constant for a photocyclization reaction in capillary microreactors using a simplified reactor model. *Reaction Chemistry & Engineering*. https://doi.org/10.1039/D4RE00087K

Lindemann, S., Bernstein, H., and Song, H.S. (2016). Engineering microbial consortia for controllable outputs. *ISME* J 10, 2077–2084 https://doi.org/10.1038/ismej.2016.26

López-Pérez, P., López-López, M., Núñez-Colín, C., Mukhtar, H., Aguilar-López, R. and Peña-Caballero, V. (2023). A novel nonlinear sliding mode observer to estimate biomass for lactic acid production. *Chemical Product and Process Modeling*, 18(4), 565-580. https://doi.org/10.1515/cppm-2021-0074

López-Pérez, P.A., Puebla, H., Velázquez S.H.I., and Aguilar-López, R. (2016). Comparison tools for parametric identification of kinetic model for ethanol production using evolutionary optimization approach. *International Journal of Chemical Reactor Engineering*, 14(6), 1201-1209. https://doi.org/10.1515/ijcre-2016-0045

Martínez-Hilario, D.G. Carrasco-Venegas, L.A., González-Fernández, J.V., Soto-Gonzales, J.L. and Carranza-Oropeza M.V. (2023). Modeling NPK nutrients release via nanoparticle/hydrogel system. *Revista Mexicana de Ingeniería Química,* 22 (2), Sim2399. https://doi.org/10.24275/rmiq/Sim2399

Pandey, S., Narayanan, I., Vinayagam, R., Selvaraj, R., Varadavenkatesan, T., and Pugazhendhi, A. (2023). A review on the effect of blue green 11 medium and its constituents on microalgal growth and lipid production. *Journal Environmental Chemistry* Engineering. 11(3), 109984. https://doi.org/10.1016/j.jece.2023.109984

Povis, A.A.L., Pérez, E.A.S., Quispe, K.A.O., and Yanqui, P.V.G. (2024). Effect of dissolved oxygen concentration on biomass production in wastewater. *Ambiente e Agua-An Interdisciplinary Journal of Applied Science*, 19, 1-11. https://doi.org/10.4136/ambi-agua.2937

Rahimikhoob, H., Sohrabi, T., and Delshad, M. (2024). Variance-based global sensitivity analysis and uncertainty quantification of the AquaCrop model parameters for basil (*Ocimum basilicum L.)* under different nitrogen fertilizer rates. *Journal of Plant Nutrition*, 47(4), 628-645. https://doi.org/10.1080/01904167.2023.2280142

Ramírez-López, C., Esparza-García, F.J., Ferrera-Cerrato, R., Alarcón, A., and Cañizares-Villanueva, R.O. (2019). Short-term effects of a photosynthetic microbial consortium and nitrogen fertilization on soil chemical properties, growth, and yield of wheat under greenhouse conditions. *Journal of Applied Phycology,* 31, 3617–3624. https://doi.org/10.1007/s10811-019-01861-2

Rao, S., Van der Schaft, A., Van Eunen, K., Bakker, B. M., and Jayawardhana, B. (2014) A model reduction method for biochemical reaction networks. *BMC Systems Biology* 8, 5 https://doi.org/10.1186/1752-0509-8-52

Rodriguez-Mata A.E., Medrano-Hermosillo J.A., Gonzalez-Huitnro, V. Djilali,A. L. Lopez-Perez, P.A., and Sonck.A. (2024). Adaptive sliding mode control of a bioreactor via nutrients variable control using a diffeomorphism. *Revista Mexicana de Ingeniería Química, 23(3), Sim24296* 23(3), https://doi.org/10.24275/rmiq/Sim24296

Raven, J.A. (2012). Carbon. In: Whitton, B. (Eds) *Ecology of Cyanobacteria II*. Springer, Dordrecht. https://doi.org/10.1007/978-94-007-3855-3_17

Renuka, N., Guldhe, A., Prasanna, R., Singh, P., and Bux, F. (2018). Microalgae as multi-functional options in modern agriculture: current trends, prospects and challenges. *Biotechnology Advances*, 36(4), 1255-1273. https://doi.org/10.1016/j.biotechadv.2018.04.004.

Reyna-Velarde, R., Cristiani-Urbina, E., Hernández-Melchor, D.J., Thalasso, F., and Cañizares-Villanueva, R.O. (2010). Hydrodynamic and mass transfer characterization of a flat-panel airlift photobioreactor with high light path. *Chemical Engineering and Processing: Process Intensification*, *49*(1), 97-103. https://doi.org/10.1016/j.cep.2009.11.014

Romero C.T., Cuervo-Parra, J.A., Robles-Olvera, J.V., Rangel C.E., and López-Pérez, P.A. (2018). Experimental and kinetic production of ethanol using mucilage juice residues from cocoa processing. *International Journal of Chemical Reactor Engineering*, 16(11), 20170262. https://doi.org/10.1515/ijcre-2017-0262

Sánchez-Zurano, A., Rodríguez-Miranda, E., Guzmán, J.L., Acién-Fernández F.G., Fernández-Sevilla J.M., and Molina Grima E. (2021). ABACO: A new model of microalgae-bacteria consortia for biological treatment of wastewaters. *Applied Sciences*. 11(3):998. https://doi.org/10.3390/app11030998

Schediwy, K., Trautmann, A., Steinweg, C., and Posten, C. (2019). Microalgal kinetics a guideline for photobioreactor design and process development. *Engineering in Life Sciences*, 19, 830-843. https://doi.org/10.1002/elsc.201900107

Scheufele, F.B., Hinterholz, C.L., Zaharieva, M.M., Najdenski, H.M., Módenes, A.N., Trigueros, D.E.G., Borba, C.E., Espinoza-Quiñones, F.R., and Kroumov, A.D. (2018). Complex mathematical analysis of photobioreactor system. *Engineering in Life Sciences* 19, 844-859. https://doi.org/10.1002/elsc.201800044

Silva, F., Nadais, H, Prates, A., Arroja, L. and Capela, I. (2009). Modelling of anaerobic treatment of evaporator condensate (EC) from a sulphite pulp mill using the IWA anaerobic digestion model no. 1 (ADM1), *Chemical Engineering Journal*, 148, 2–3. https://doi.org/10.1016/j.cej.2008.09.002

Solimeno, A., Samsó, R., Uggetti, E., Sialve, B., Steyer, J. P., Gabarró, A., and García, J. (2015). New mechanistic model to simulate microalgae growth, *Algal Research* 12, 350-358. https://doi.org/10.1016/j.algal.2015.09.008

Song H. S. (2018). Design Principles of Microbial Communities: From Understanding to Engineering. *Current Genomics* 19:699–700

Song H. S., Cannon W. R., Beliaev A. S., and Konopka A. (2014). Mathematical modeling of microbial community dynamics: a methodological review. *Processes* 2:711–752. https://doi.org/10.3390/pr2040711

Song H., Lee N., Kessell A. K., McCullough H. C., Park S., Zhou K., Lee D. (2024). Kinetics-based inference of environment-dependent microbial interactions and their dynamic variation. *mSystems* 9: e01305-23. https://doi.org/10.1128/msystems.01305-23

Tredici M. R. (2004). Mass production of microalgae: photobioreactors. In *Handbook of Microalgal Culture: Biotechnology and Applied Phycology.* Richmond, A. (Ed.) Blackwell Science Ltd. Oxford. 178-214. https://doi.org/10.1002/9781118567166

Touloupakis, E., Zittelli, G.C., and Benavides, A.M.S. (2023). Growth and photosynthetic performance of *Nostoc linckia* (formerly *N. calcicola*) cells grown in BG11 and $BG11_0$ media. *Photochemical and Photobiological Sciencies,* 22, 795–807 https://doi.org/10.1007/s43630-022-00353-6